Separation Science and Technology
Publication details, including instructions for authors and subscription information:
http://www.informaworld.com/smpp/title~content=t713708471

A PREDICTIVE MODEL FOR ULTRAFILTRATION: COMBINATION OF OSMOTIC PRESSURE MODEL AND IRREVERSIBLE THERMODYNAMICS

Sandeep K. Karode[a]
[a] MEDAL LP, Newport, DE, U.S.A.

Online publication date: 30 November 2001

To cite this Article Karode, Sandeep K.(2001) 'A PREDICTIVE MODEL FOR ULTRAFILTRATION: COMBINATION OF OSMOTIC PRESSURE MODEL AND IRREVERSIBLE THERMODYNAMICS', Separation Science and Technology, 36: 12, 2659 — 2676
To link to this Article: DOI: 10.1081/SS-100107218
URL: http://dx.doi.org/10.1081/SS-100107218

SEPARATION SCIENCE AND TECHNOLOGY, 36(12), 2659–2676 (2001)

A PREDICTIVE MODEL FOR ULTRAFILTRATION: COMBINATION OF OSMOTIC PRESSURE MODEL AND IRREVERSIBLE THERMODYNAMICS

Sandeep K. Karode*

Water Treatment Division, Thermax Ltd,
15 Mumbai Pune Road, Wakdewadi,
Pune 411 003, India

ABSTRACT

An unsteady state model for ultrafiltration that describes transport within the pores of the ultrafiltration membrane is presented. The new, improved model combines the osmotic pressure model for transport in the polarization layer and the irreversible thermodynamics approach. The model is capable of simultaneously predicting 1) the permeate flux, 2) the permeate concentration, and 3) the concentration at the membrane feed surface when all the transport parameters are fixed. The model data are comparable to the experimental data cited in the literature. Model simulations conducted by varying 1 parameter while the others are kept constant show that the entire range of observed transmissions is a function of permeate flux. For certain parameter values, the model predicts observed transmission greater than unity. Hence, in principle, an ultrafiltration system in which the product of interest is concentrated in the permeate stream can be designed. The model also correctly pre-

*Current address: MEDAL LP, 305 Water Street, Newport, DE 19804. Fax: +(91) (20) 518 0236; E-mail: sandeepkarode@yahoo.com

dicts the experimental observation that the magnitude of observed transmission that is greater than unity decreases as the feed concentration increases.

Key Words: Osmotic pressure; Irreversible thermodynamics; Model; Unsteady state; Ultrafiltration; Protein

INTRODUCTION

Membrane ultrafiltration has elicited considerable interest in recent years because it has become an increasingly important separation process for proteins. Much work has been directed toward understanding the interactions between the membrane and the protein (1,2). However, in a large majority of cases, the membrane used is either totally retentive or completely permeable to the protein being subjected to ultrafiltration. The use of partially retentive membranes have the possible advantage of concentrating the protein in the permeate stream where the observed transmission ($\tau_o = C_p/C_f$) is greater than unity. This phenomenon, though rare, has been reported for both unsteady state (3) and steady state (4) operating conditions. Yet, relatively little understanding exists on the theoretical physics of this process.

Over the years, the transport through porous membranes has been modeled based on 3 basic approaches: the Kedem-Katchalsky approach based on irreversible thermodynamics (5,6), the Stefan-Maxwell multicomponent diffusion Eqs. (7–9); and hydrodynamic models (10,11). Each of these approaches, based on various levels of mathematical rigor, model the transport through the pores as a combination of diffusive and convective transport.

Transmembrane permeation based on boundary layer phenomena has been modeled historically in 3 ways: the osmotic pressure model (12,13); the boundary-layer resistance model (14); and the gel-polarization model (15). Song and Elimelech (16) developed a steady state theory for concentration polarization in which the solute is modeled as a hard sphere. They show that the permeate flux is characterized by a dimensionless filtration number and that for filtration numbers less than 15, one cannot expect the formation of a cake (or gel) layer of rejected particles on the surface of the membrane. This work was then extended by Song (17) to estimate the limiting flux in ultrafiltration. In 1998, Elimelech and Bhattacharjee (18) furthered this approach by developing a model based on the equivalence of the osmotic pressure model and filtration theory.

The researchers in all the cited literature rigorously modeled either the transport through the pore or the phenomena occurring in the boundary layer. Very little attempt had been made to couple the 2 approaches. In a 1999 short communication, an unsteady state model was presented in which an attempt was made to couple the 2 approaches (19). The feed surface concentration was not assumed to

MARCEL DEKKER, INC.
270 Madison Avenue, New York, New York 10016

be constant, and the permeate flux and the permeate concentration were predicted by the model. The transport through the pore was assumed to be characterized by an overall, lumped, transport parameter that was assumed to be diffusive in nature. With such an approach, it was shown that for a certain range of parameters, it was possible to explain transmission greater than unity.

We improve on the model proposed by Karode (19) by modeling the boundary layer phenomena based on the osmotic pressure model and the transport through the pore based on the irreversible thermodynamic approach of Kedem and Ketchalsky (5). The improved model is consistent with experimental data for BSA (Bovine Serum Albumin) ultrafiltration using partially retentive polyethersulfone 100-K membranes in a stirred ultrafiltration device (20). In their work, Opong and Zydney (20) evaluated the relative contributions of diffusive and convective transport to the overall protein flux. They evaluated the membrane feed-surface concentration using a stagnant film model and hence were able to report the actual protein transmission ($\tau = C_p/C_w$).

After the improved model is compared against experimental data, some model predictions are presented. The presented model is capable of predicting the entire range of observed transmission as a function of the permeate flux. Operating conditions for transmission greater than unity are also presented and discussed.

THEORY

In ultrafiltration, the formation of a concentration polarization layer (Fig. 1) can be described by

$$\frac{\partial C}{\partial t} = -v\frac{\partial C}{\partial x} + D_b\frac{\partial^2 C}{\partial x^2} \tag{1}$$

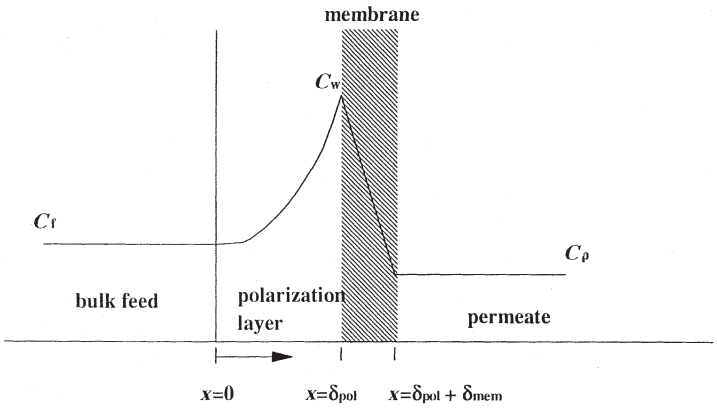

Figure 1. Schematic of a concentration polarization layer.

with the following initial and boundary conditions:

$$t = 0 : 0 \le x \le \delta_{pol};\ C = C_f \tag{2a}$$

$$t > 0 : x = 0;\ C = C_f \tag{2b}$$

$$t > 0 : x = \delta_{pol};\ vC = D_b \left.\frac{\partial C}{\partial x}\right|_{\delta_{pol}^-} - \varepsilon D_m \left.\frac{\partial C}{\partial x}\right|_{\delta_{pol}^+} + (1 - \sigma) v \left(\frac{C}{K}\right) \tag{2c}$$

The boundary condition at $x = \delta_{pol}$ is derived from a continuity of flux. In Eq. (2c), the solute transport within the pore is modeled based on the irreversible thermodynamics model (5). Here D_m is the diffusion coefficient for the protein through the pore of the microporous membrane. In the earlier model (19), D_m was assumed to be a lumped parameter incorporating the combined effects of hindered diffusion, affinity between the protein and membrane surface, and the contribution due to convective transport.

In Eq. (2c), K is a partition coefficient defined as a ratio of the solute concentration at the membrane surface in the feed to that in the membrane pore. K would is a function of the electrostatic interactions between the protein and the membrane and also a function of steric effects. σ is the reflection coefficient, which according to the classical work of Staverman (21) is 0 for a completely permeable membrane and unity for an ideally retentive membrane. In the words of Staverman, "In intermediate cases $(1 - \sigma)$ is the ratio of solute concentrations in a sample before and after flowing through the membrane respectively." Mathematically, using the symbols used the present work, this can be written as

$$1 - \sigma = \frac{C_{\delta_{pol\,+\,mem}}}{C_{\delta_{pol}}}$$

Extending the arguments of Spiegler and Kedem (6) to unsteady state conditions, we can write the governing equation within the membrane ($\delta_{pol} < x < \delta_{pol} + \delta_{mem}$) as

$$\frac{\partial C}{\partial t} = D_m \frac{\partial^2 C}{\partial x^2} - (1 - \sigma) \frac{v}{\varepsilon} \frac{\partial C}{\partial x} \tag{3}$$

along with the following initial and boundary conditions:

$$t = 0 : \delta_{pol} < x \le \delta_{pol} + \delta_{mem};\ C = 0 \tag{4a}$$

$$t > 0 : x = \delta_{pol};\ vC = D_b \left.\frac{\partial C}{\partial x}\right|_{\delta_{pol}^-} - \varepsilon D_m \left.\frac{\partial C}{\partial x}\right|_{\delta_{pol}^+} + (1 - \sigma) v \left(\frac{C}{K}\right) \tag{4b}$$

$$t > 0 : x = \delta_{pol} + \delta_{mem};\ -\varepsilon D_m \left.\frac{\partial C}{\partial x}\right|_{\delta_{pol\,+\,mem}} + (1 - \sigma) vC = vC \tag{4c}$$

In asymmetric ultrafiltration membranes, the pore size gradually changes as the membrane skin layer merges into the underlying support layer. Therefore, the environment that a solute molecule enters as it exits the skin layer does not abruptly change. Hence, a partition coefficient need not be introduced into Eq. (4c).

Based on the osmotic pressure model, the permeate flux is given by

$$v = \frac{\Delta P - \Delta\pi}{\mu(R_m + R_a)} = \frac{\Delta P - \Delta\pi}{\mu R_{ma}} \tag{5}$$

$\Delta\pi$ is the osmotic pressure at the feed surface (π_{pol}) of the membrane minus the osmotic pressure at the permeate surface ($\pi_{pol\,+\,mem}$) of the membrane, and R_m and R_a are the resistances offered by the clean membrane and due to adsorption of the protein on the membrane, respectively.

Osmotic pressure as a function of protein concentration is given by (22)

$$\pi = \frac{RT}{M}(C + A_2C^2 + A_3C^3) \tag{6}$$

where R is the gas constant; T is the temperature; and M is the molecular weight of the protein. A_2 and A_3 are the second and third virial coefficients respectively.

Equations (1–6) were nondimensionalized as follows:

$$C^* = \frac{C}{C_f};\ x^* = \frac{x}{\delta_{pol}};\ t^* = \frac{D_b t}{\delta_{pol}^2} \tag{7}$$

After they were nondimensionalized, Eqs. (1–6) were solved through a finite difference scheme (23) to predict the permeate concentration and the permeate flux as a function of time and the concentration in the polarization layer and through the membrane as a function of spatial distance. The nondimensional boundary-layer thickness was discretized into 100 equally spaced intervals such that $x^* = 0$ corresponded to the grid point number 1 and $x^* = 1$ corresponded to grid point number 101. The membrane was discretized into 20 equally spaced intervals. By discretizing Eq. (1) through the central finite-difference method (23), 99 first-order ordinary differential equations (I-ODEs) were solved for the concentration profile within the polarization layer. Similarly, discretization of Eq. (3) resulted in 19 I-ODEs for the concentration profile within the membrane.

Discretizing Eq. (2c) then resulted in a nonlinear algebraic equation to be solved for the membrane feed-surface concentration $C^*\big|_{x^*=1} = C^*_m$. This was solved by the Newton-Raphson method (23). A similar nonlinear equation that represented the permeate face of the membrane was a result of the discretization of Eq. (4c). This too was solved using the Newton-Raphson method (23).

MARCEL DEKKER, INC.
270 Madison Avenue, New York, New York 10016

DISCUSSION

Model Comparison with Literature Experimental Data

Table 1 gives the model parameters for BSA ultrafiltration data reported by Opong and Zydney (20). The model was fit to experimental data for a feed concentration (C_f) of 5 kg/m^3. The diffusivity in the polarization layer (D_b) was estimated using the following correlation (24):

$$D_b = \frac{2.75 \times 10^{-9}}{M^{1/3}} \tag{8}$$

For BSA (molecular weight 67 kda), the D_b value was close to the one estimated by Opong and Zydney (6.7×10^{-11} m^2/s) reported in Table 1. The mass transfer coefficient (k) for the stirred cell used in the ultrafiltration studies was reported as 5.2×10^{-6} m/s. This was used to calculate the polarization boundary layer thickness ($\delta_{pol} = D_b/k$). The membrane skin layer thickness was 0.5 μm. The membrane resistance was calculated using the reported hydraulic permeability of 2×10^{-12} m and the viscosity (μ) given in Table 1. The virial coefficients for calculating the BSA osmotic pressure were also reported by Opong and Zydney (20). Though the manufacturer of the membranes used in their studies reported a surface porosity of 0.8, Opong and Zydney reported that the porosity after protein adsorption was approximately 0.5.

The model was fit to experimental $\tau_o - v$ data (20) by varying the feed pressure (ΔP), K, and D_m. The model fit to the experimental data for physically realistic values of feed pressure and D_m resulted in $K \approx 1$. A sensitivity analysis showed that the model predictions were far more sensitive to D_m than to K. Best fit values for the model parameters are shown in Table 1.

Table 1. Model Parameters for BSA Ultrafiltration

Parameter	Value
C_f	5 kg/m^3
D_b	6.75×10^{-11} m^2/s
D_m	1×10^{-13} m^2/s
K	1.0
ΔP	0–50 kPa
R_{ma}	5×10^{11} m^{-1}
δ_{pol}	1.29×10^{-5} m
δ_{mem}	0.5×10^{-6} m
ε	0.5
π	$(RT/M)(C + 9.22 \times 10^{-3}C^2 + 3.01 \times 10^{-5}C^3)$ Pa
μ	10^{-3} Pa·s

MARCEL DEKKER, INC.
270 Madison Avenue, New York, New York 10016

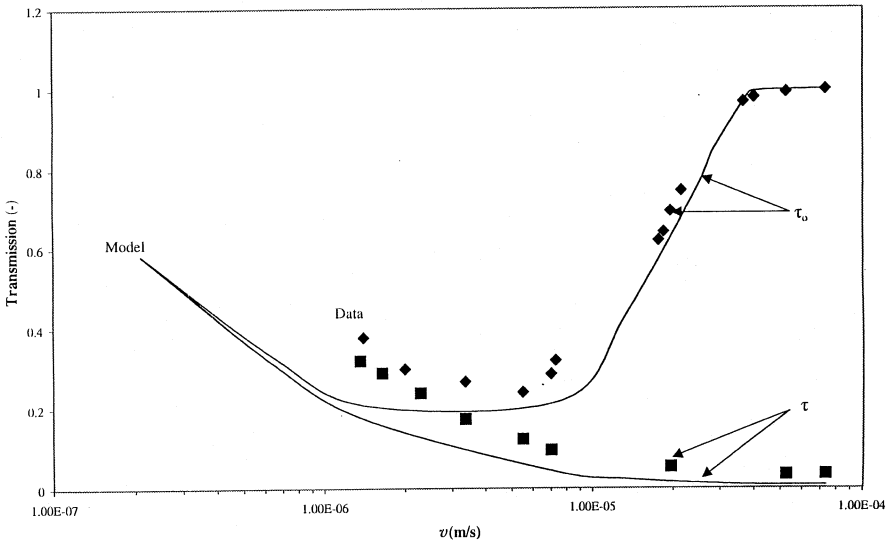

Figure 2. Model fit to experimental data of Opong and Zydney (20) with model parameters given in Table 1.

Figure 2 shows that the steady state model fit to the experimental data of Opong and Zydney (20) for a constant value of $D_m = 1 \times 1\,0^{-13}$ m^2/s. This would correspond to the value of hindered diffusion of BSA (67 kd) with the pores of the OMEGA 100-K ultrafiltration membranes of molecular weight cutoff value (MWCO) $\approx$ 100 kd. Because the permeate flux in Fig. 2 is plotted on a logarithmic scale, a slight discrepancy between the model predictions and the experimental data seem magnified on the logarithmic plot. As can be seen from Fig. 3, the model effectively captures the minimum in τ_o as a function of v for low values of v and also correctly predicts a decreasing trend of τ with increasing v. Because the D_m value is fixed, the permeate flux (v), the permeate concentration (C_p), and the concentration at the (feed) membrane surface (C_w) are predicted simultaneously. Furthermore, model prediction of the τ-v profile is in good agreement with that calculated by Opong and Zydney (20) who used a stagnant film model. However, unlike in the stagnant film model, a constant concentration at the feed surface of the membrane is not assumed in the current model.

Model Predictions

After verifying that the model data were comparable to literature experimental data, some of the predictions of this improved model will be presented. In these simulations, 1 parameter has been varied while all other parameters were held constant at the indicated values.

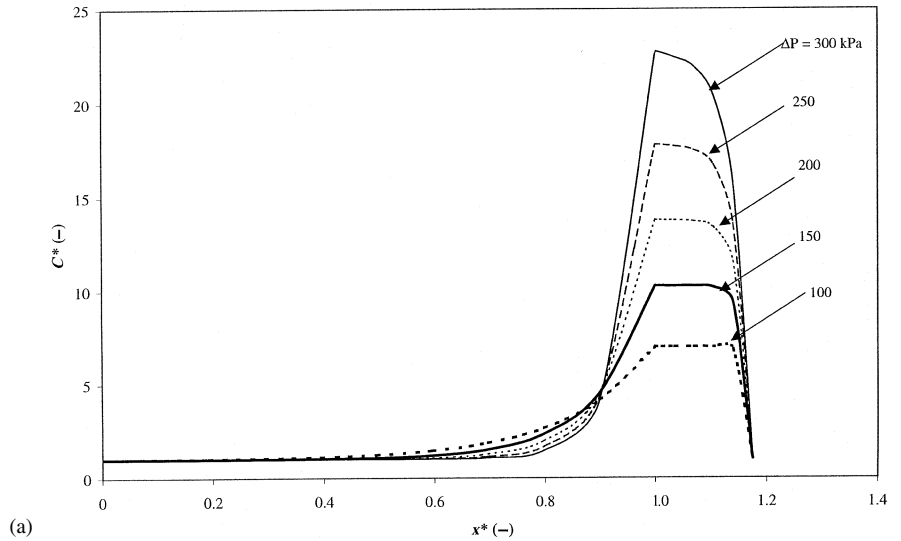

(a)

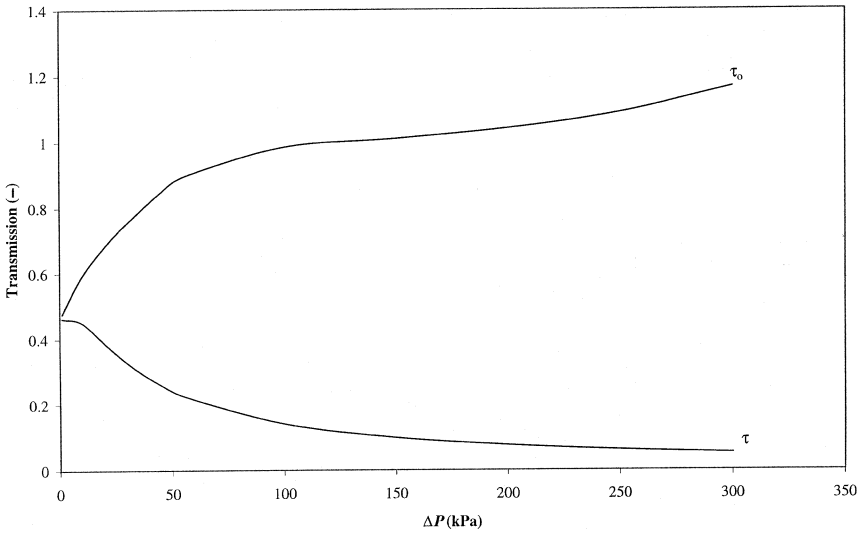

(b)

Figure 3. Model prediction of (a) nondimensional concentration profile in the polarization layer and through the membrane and (b) transmission for various values of applied pressure (model parameters given in the text).

MARCEL DEKKER, INC.
270 Madison Avenue, New York, New York 10016

Effect of Pressure

Figures 3a and 3b show the effect of the applied pressure (ΔP) for constant feed concentration, $C_f = 0.2\ kg/m^3$, a membrane resistance (R_{ma}) of $7 \times 10^{11}\ m^{-1}$, and a membrane thickness (δ_{mem}) of 1 μm (other parameters were as listed in Table 1).

Figure 3a shows the model prediction of the steady-state nondimensional concentration profile for various values of ΔP. As the applied pressure increased, membrane (feed) surface concentration also increased. Though an almost proportional increase in the surface concentration existed, the nondimensional permeate concentration ($C_p/C_f = \tau_o$) was not proportional (Fig. 3b). As a consequence, the true transmission ($\tau = C_p/C_w$) decreased as a function of increased applied pressure. During the model simulations, the filtration number defined by Song and Elimelech (16) was verified as always less than 15, which indicates the absence of a gel layer on the surface of the membrane. In the absence of the gel layer, the concentration on the feed surface of the membrane is expected to increase as a function of applied pressure.

For low applied pressures, the permeate flux was proportionally lowered. Hence, the rate of transport of material toward the membrane surface was also lower. Consequently, the membrane surface concentration was not substantially different from the bulk feed concentration and τ was almost equal to τ_o (Fig. 3b). As ΔP increased, τ_o also increased, though at progressively lower rates. As ΔP increased above a critical value, τ_o became greater than unity. However, the true transmission τ was far less than unity. Hence, for partially retentive membranes, for high enough values of applied pressure, the steady-state observed transmission is greater than unity.

Balakrishnan, Agarwal, and Cooney (4) discussed the possibility of such steady-state observed transmission being greater than unity. They suggested the use of a modified-concentration polarization model to explain this phenomenon. In such a development, an additional transport term is added to the concentration polarization model, which according to Balakrishnan, Agawal, and Cooney accounts for additional flux due to electrostatic interactions between the protein and the membrane. However, for identical operating conditions using membranes of the same material but of different MWCO values, they were forced to change the magnitude of this additional transport term to explain the experimental results. The improved model presented is able to explain the experimentally observed trends.

Effect of Hindered Diffusion Coefficient

Figure 4 shows the effect of the diffusivity within the membrane pores (D_m) for the same feed concentration, membrane resistance, and membrane thickness

MARCEL DEKKER, INC.
270 Madison Avenue, New York, New York 10016

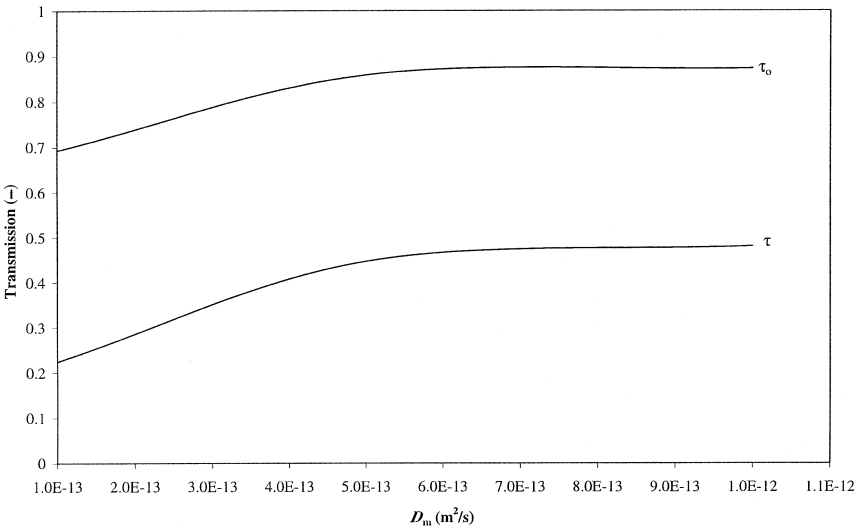

Figure 4. Model prediction of transmission as a function of diffusivity within the membrane pores (model parameters given in the text).

reported for the concentration profiles and transmission prediction previously described. The applied pressure was set to 30 kPa and the other model parameters were as listed in Table 1.

D_m depends on the size of the protein molecule and the size of the pores in the ultrafiltration membrane. A tighter membrane (lower MWCO) is expected to lead to a low D_m, and as the MWCO of the membrane increases, D_m is also expected to increase.

As can be seen from Fig. 4, when all other parameters were kept constant, an increase in D_m resulted in increased observed transmission and true transmission values. Such an effect of the MWCO on observed transmission was reported by Balakrishnan, Agarwal, and Cooney (4) when they first reported that the experimental steady-state observed transmission was greater than unity when a vortex filter was used.

Effect of Membrane Resistance

Figures 5a, 5b, 5c show the effect of the membrane resistance (R_{ma}) for constant feed concentration, $C_f = 1$ kg/m^3, a diffusivity within the membrane of $D_m = 1 \times 10^{-13}$ m^2/s, and an applied pressure of 100 kPa. The other parameters were identical to those in D_m modeling.

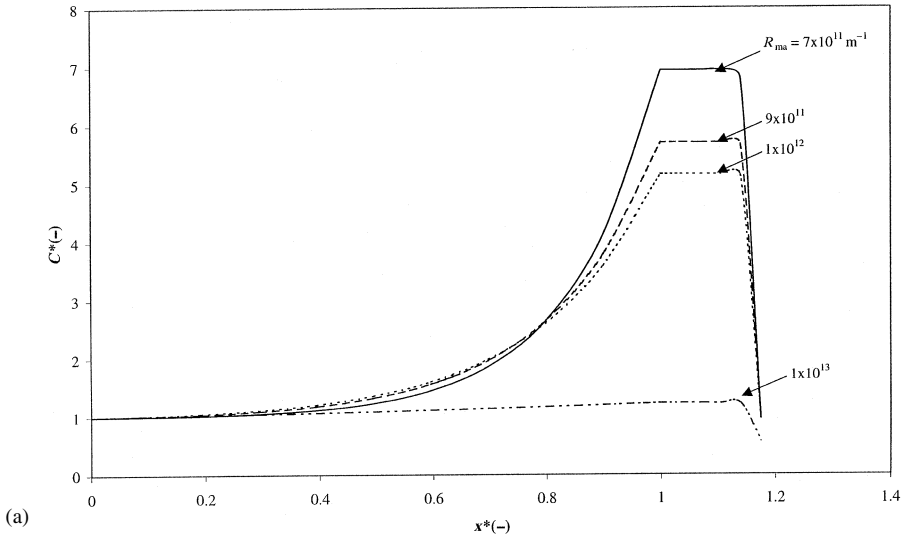

(a)

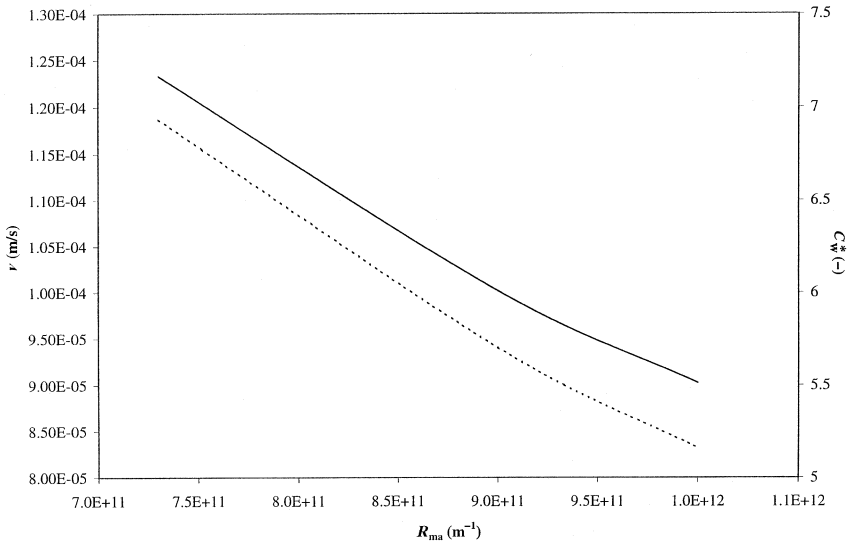

(b)

Figure 5. Model prediction of (a) nondimensional concentration profile in the polarization layer and through the membrane; (b) flux vs. membrane resistance (solid line) and nondimensional wall concentration vs. membrane resistance (dashed line); (c) transmission vs. flux for various values of membrane resistance (model parameters given in the text).

(continued)

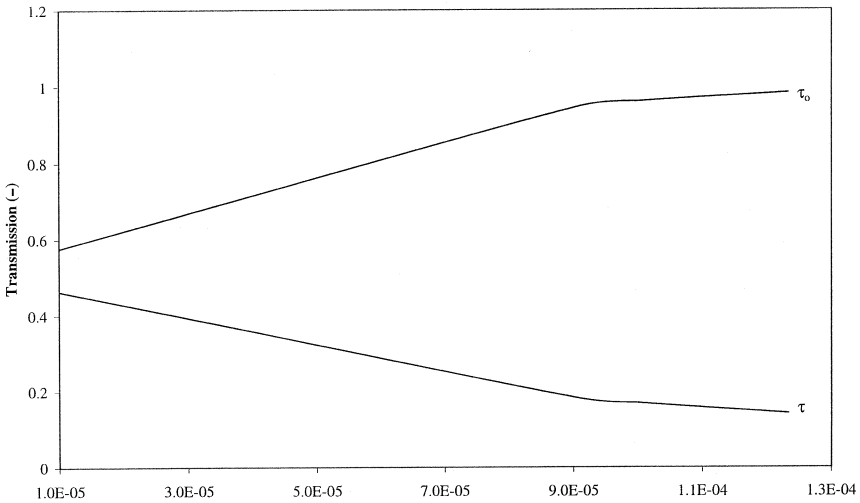

(c)

Figure 5. Continued.

Figure 5a shows the nondimensional concentration profile for various values of R_{ma}. As the membrane resistance decreases when all other parameters are held constant, the wall concentration increases. This result is found because a decrease in membrane resistance led to a corresponding increase in permeate flux. Hence, as shown in Fig. 5b, an increase in permeate flux leads to increased transport of material toward the membrane surface, which leads to a corresponding increase in membrane feed-surface concentration.

The corresponding effect on observed and true transmission can be seen in Fig. 5c. As the permeate flux increased (i.e., the membrane resistance decreased), the membrane feed-surface concentration became much higher than the bulk feed concentration. Hence, τ_o increased and τ decreased as the membrane resistance decreased (i.e., as the permeate flux increased).

Effect of Feed Concentration

Figure 6a shows the effect of feed concentration on the permeate flux as a function of applied pressure for $D_m = 1 \times 10^{-13}$ m^2/s with other parameters identical to those in the effect of hindered diffusion coefficients modeling. As expected, for a fixed applied pressure, the permeate flux decreased with an increase in feed concentration.

Figure 6b shows the effect of concentration on τ_o and τ for a fixed applied pressure (100 kPa). As can be seen from the figure, an increase in feed concentra-

Marcel Dekker, Inc.
270 Madison Avenue, New York, New York 10016

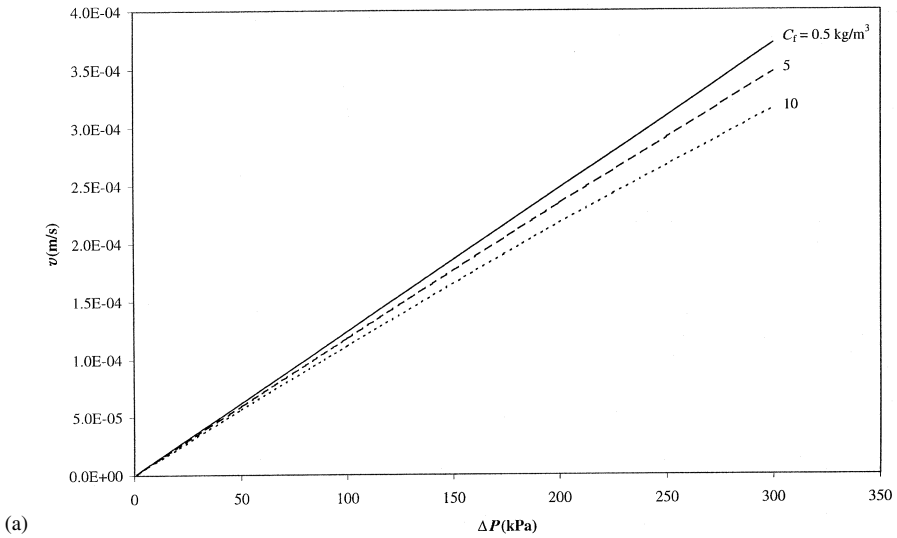

(a)

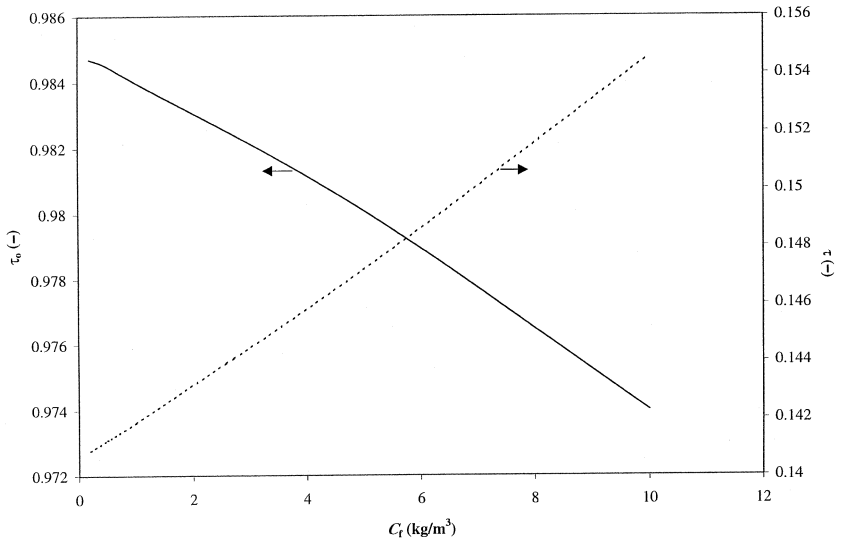

(b)

Figure 6. Model prediction of (a) flux vs. transmembrane pressure difference, (b) transmission vs. bulk feed concentration, (c) transmission vs. transmembrane pressure difference for various values of feed concentration (model parameters given in the text).

(continued)

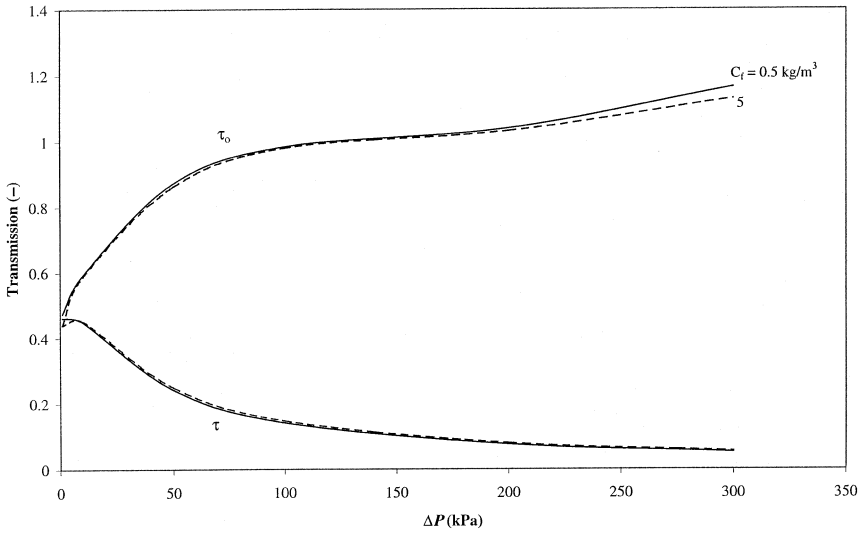

(c)

Figure 6. Continued.

tion led to a decrease in observed transmission and a corresponding increase in true transmission. This prediction corresponds with several experimental results on protein transmission.

Figure 6c shows the effect of applied pressure on transmission for 2 feed concentrations, 0.5 kg/m^3 and 5.0 kg/m^3. As can be seen from the figure, the model predicts a decrease in the magnitude of observed transmission with increasing feed concentrations at all applied pressures. The true transmission however increases with feed concentration. This prediction is consistent with several experimental results. The observed transmission should approach a limiting value for very high applied pressures. However, in the simulations, the applied pressure was restricted to 0–350 kPa because for higher pressures, the filtration numbers defined by Song and Elimelech (16) were close to 15.

As shown by the cross-flow filtration theory of Song and Elimelech (16), for filtration numbers greater than 15, some additional physics must be built into the model to account for an addition in the permeation resistance due to a gel (cake) layer of rejected particles.

Effect of Partition Coefficient

Figure 7 shows the effect of the feed-side partition coefficient on the observed transmission when all other parameters were kept constant. As expected, the observed transmission (τ_o) decreased as K increased. At very high values of K,

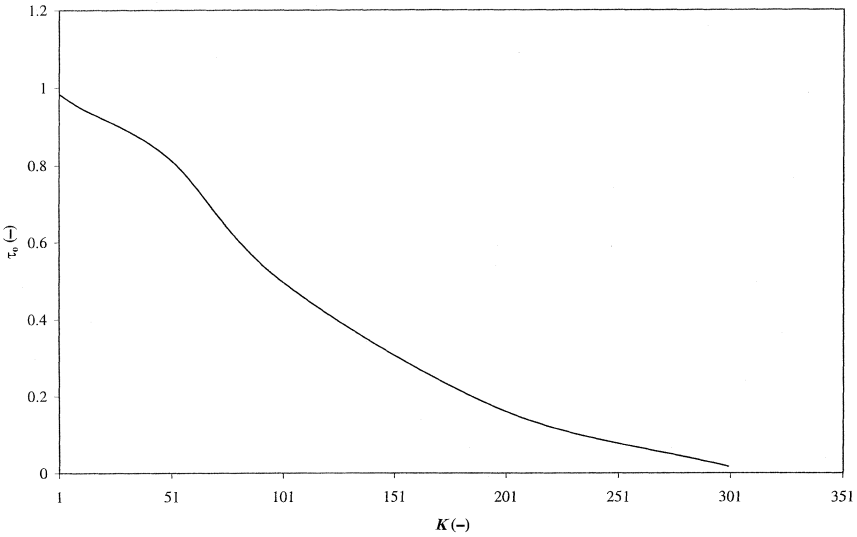

Figure 7. Model prediction of observed transmission (τ_o) vs. feed side partition coefficient (K) (model parameters given in the text).

the observed rejection becomes independent of the other parameters, such as D_m and ΔP, and the membrane behaves like an ideal filter with observed transmission values of 0.

The predictions presented are based on the set of model parameters used to fit experimental data reported by Opong and Zydney (20) and are given in Table 1. These simulations can be used as an indicator of the effect of system variables on membrane performance. For quantitative predictions, model parameters must be estimated for specific cases and then simulations run using the model presented in this work.

CONCLUSIONS

The data from the improved unsteady-state model for ultrafiltration that combines the osmotic pressure model and the irreversible thermodynamics model was consistent with experimental protein ultrafiltration data. The model simultaneously predicts the steady-state permeate flux and concentration along with the concentration at the membrane feed surface. No implicit assumptions are made regarding the constancy of the membrane feed-surface concentration.

The model predicts that at low applied pressures, the observed transmission, τ_o (defined as the ratio of the permeate concentration to the bulk feed concentration) is almost equal to the true transmission, τ (defined as the ratio of the perme-

ate concentration to the concentration at the membrane feed surface). As the applied pressure increases, τ_o increases while τ decreases.

With increasing diffusivity within the membrane, at constant applied pressure, both τ_o and τ increase. However, the increase tends to level off at high values of D_m. Hence, theoretical protein ultrafiltration systems that utilize partially retentive membranes to create protein concentration in the permeate stream could be designed.

The model also predicts that with decreasing feed concentration, the magnitude of observed transmission greater than unity increases, a result that was also seen from experiments by Balakrishnan, Agarwal, and Cooney (4). This result means that any industrial ultrafiltration system that is designed to concentrate the protein into the permeate should be operated in a multipass mode (only the retentate stream being recycled into the feed tank). In such an installation, the permeate stream would be progressively concentrated to a greater extent, which would lead to efficient concentration of the protein.

An increase in the membrane resistance (R_{ma}) leads to a decrease in the permeate flux and in the membrane feed-surface concentration. The corresponding observed transmission is predicted to decrease while the true transmission is predicted to increase.

Based on the model predictions, the observed transmission (or the membrane rejection defined as $R_o = 1 - \tau_o$) is found to be controlled by the transport parameters within the polarization layer and within the membrane pores. Hence, for a given membrane material, by varying the system parameters (such mass transfer coefficient and applied pressure), a wide variation in the observed and true transmission values can be found.

NOMENCLATURE

A_j	virial coefficient, $j=1,2,3$ ($Pa \cdot m^{3j}/kg^j$)
C	concentration (kg/m^3)
D_b	diffusion coefficient in polarization boundary layer (m^2/s)
D_m	hindered diffusion coefficient in the membrane pores (m^2/s)
k	mass transfer coefficient (m/s)
K	partition coefficient (C_w^-/C_w^+) (−)
M	averaged molecular weight (d)
ΔP	transmembrane pressure difference (Pa)
R_a	resistance due to adsorption (m^{-1})
R_m	membrane resistance (m^{-1})
R_{ma}	($R_m + R_a$) (m^{-1})
t	time (s)
v	permeate flux (m/s)
x	coordinate perpendicular to the membrane (m)

MARCEL DEKKER, INC.
270 Madison Avenue, New York, New York 10016

Greek Letters

δ	thickness (m)
ε	membrane surface porosity
μ	dynamic viscosity (Pa·s)
π	osmotic pressure (Pa) (−)
σ	reflection coefficient ($1 - C_p/C_f$) (−)
τ_o	observed transmission (C_p/C_f) (−)
τ	true transmission (C_p/C_w) (−)

Indices

b	boundary (polarization) layer
f	bulk feed
mem	membrane
o	observed
p	permeate
pol	polarization layer
w	membrane feed surface
*	nondimensional
+	in the membrane pore
−	in the polarization layer

REFERENCES

1. Balakrishnan, M.; Agarwal, G.P. Protein Fractionation in a Vortex Flow Filter I: Effect of System Hydrodynamics and Solution Environment on Single Protein Transmission. J. Memb. Sci. **1996,** *112,* 47–74.
2. Musale, D.A.; Kulkarni, S.S. Effect of Membrane Solute Interactions on Ultrafiltration Performance. J. Macromol. Sci. Rev. Macromol. Chem. Phys. **1998,** *C38* (4), 615–636.
3. Le, M.S.; Howell, J.A. An Alternative Model for Ultrafiltration. Chem. Eng. Res. Des. **1984,** *62,* 373–380.
4. Balakrishnan, M.; Agarwal, G.P.; Cooney, C.L. Study of Protein Transmission through Ultrafiltration Membranes. J. Memb. Sci. **1993,** *85,* 111–128.
5. Kedem, O.; Ketchalsky, A. Thermodynamic Analysis of Permeability of Biological Membranes to Non-electrolytes. Biochim. Biophys. Acta **1958,** *27,* 229–246.
6. Spiegler, K.S.; Kedem, O. Thermodynamics of Hyperfiltration (Reverse Osmosis): Criteria for Efficient Membranes. Desalination **1966,** *1,* 311–326.
7. Lightfoot, E.N. *Transport phenomena in living systems*; Wiley: New York, 1974.

MARCEL DEKKER, INC.
270 Madison Avenue, New York, New York 10016

8. Robertson, B.C.; Zydney, A.L. Stefan-Maxwell Analysis of Protein Transport in Porous Membranes. Sep. Sci. Technol. **1988,** *23*, 1799–1811.
9. Bellara, S.R.; Cui, Z. A Maxwell-Stefan Approach to Modeling the Cross Flow Ultrafiltration of Protein Solutions in Tubular Membranes. Chem. Eng. Sci. **1998,** *53* (12), 2153–2166.
10. Anderson, J.L.; Quinn, J.A. Restricted Transport in Small Pores: A Model for Steric Exclusion and Hindered Particle Motion. Biophys. J. **1974,** *14,* 130–150.
11. Deen, W.M. Hindered Transport of Large Molecules in Liquid Filled Pores. AIChE J. **1987,** *33,* 1409–1425.
12. Goldsmith, R.L. Macromolecular Ultrafiltration with Microporous Membranes. Ind. Eng. Chem. Res. **1971,** *10,* 113–120.
13. Kozinsky, A.A.; Lightfoot, E.N. Protein Ultrafiltration: A General Example of Boundary Layer Filtration. AIChE J. **1972,** *18,* 1030–1040.
14. Wijmans, J.G.; Nakao, S.; van den Berg, J.W.A.; Troelstra, F.R.; Smolders, C.A. Hydrodynamic Resistance of Concentration Polarization Boundary Layers in Ultrafiltration. J. Memb. Sci. **1985,** *22,* 117–135.
15. Baltt, W.F.; Dravid, A.; Michaels, A.S.; Nelsen, L.M. Solute polarization and cake formation in membrane ultrafiltration: causes, consequences and control techniques, in Flinn, J.E. Ed. Plenum Press: New York, 1970; 47.
16. Song, L.; Elimelech, M. Theory of concentration polarization in crossflow filtration. J. Chem. Soc. Farady Trans. **1995,** *91* (19), 3389–3398.
17. Song, L. A new model for the calculation of limiting flux in ultrafiltration. J. Memb. Sci. **1998,** *144,* 173–185.
18. Elimelech, M.; Bhattacharjee, S. A novel approach for modeling concentration polarization in crossflow membrane filtration based on the equivalence of osmotic pressure model and filtration theory. J. Memb. Sci. **1998,** *145,* 223–241.
19. Karode, S.K. A new unsteady state model for macromolecular ultrafiltration. Chem. Eng. Sci. **1999,** *55,* 1769–1773.
20. Opong, W.S.; Zydney, A.L. Diffusive and convective protein transport through asymmetric membranes. AIChE J. **1991,** *37* (10), 1497–1510.
21. Staverman, A.J. The theory of measurement of osmotic pressure. Rec. Trav. Chim. **1951,** *70,* 344–352.
22. Vilker, V.L.; Colton, C.K.; Smith, K.A. The osmotic pressure of concentrated protein solutions: Effects of concentration and pH in saline solutions of Bovine Serum Albumin. J. Colloid Interf. Sci. **1981,** *79,* 548–566.
23. Press, W.H.; Flanerry, B.P.; Teukolsky, S.A.; Vetterling, W.T. Numerical recipes: The art of scientific computing. Cambridge University Press: Cambridge, 1990.
24. Sherwood, T.K.; Pigford, R.L.; and Wilke, C.R. *Mass Transfer.* McGraw-Hill: New York, 1975.

Received May 2000
Revised November 2000

Request Permission or Order Reprints Instantly!